Sun *et al. Biochar* (2026) 8:69
https://doi.org/10.1007/s42773-025-00547-y

Biochar

ORIGINAL RESEARCH Open Access

Hydrochar as an effective amendment for enhancing soil aggregation and carbon sequestration: evidence from comparative microcosm experiments

Liyang Sun[1], Jim J. Wang[2], Sun Wei[3,4], Pingping Ye[1], Yue Deng[1], Xiangtian Meng[3,4], Ronghua Li[3,4], Zongsheng Zhang[5], Xiaoxuan Su[1*] and Ran Xiao[1*]

Abstract

Enhancing soil organic carbon (SOC) and aggregate stability is pivotal for maintaining soil health and ensuring agricultural sustainability. However, conventional organic amendments often exhibit suboptimal efficiency in achieving these goals. Hydrochar, synthesized via hydrothermal carbonization (HTC), offers a promising solution by integrating labile and recalcitrant carbon fractions to synergistically address these challenges. However, its mechanisms of action remain not fully understood. In the present study, a microcosmic incubation experiment was conducted to evaluate the short-term impacts of hydrochar on SOC sequestration and soil aggregation in comparison with biochar and straw in a purple soil (*Entisol*). Hydrochars derived from maize straw (SH), pig manure (PH), and *Zanthoxylum* stalks (HH) were also compared to assess feedstock-driven variability. The results demonstrated the superior performance of hydrochars, particularly those derived from *Zanthoxylum* stalks, which significantly increased the mean weight diameter (MWD) by 70–100% and SOC content by 143–149%, outperforming biochar and straw. Specifically, hydrochar-originated carbon persisted primarily as particulate organic matter (POM) and accumulated in macro-aggregate, while shifts in microbial communities contributed to SOC stabilization. In comparison, soil aggregation was driven by labile carbon fractions (e.g., dissolved organic carbon, DOC) and soil microorganisms, specifically *Actinobacteria* and *Ascomycota*. Feedstock properties, such as the C/N ratio and lignin content, modulated the effectiveness of hydrochar as a soil amendment. Notably, stalk-derived hydrochar exhibited superior carbon retention (12% total carbon loss vs. 30–44% for other amendments) and aggregate stability due to its recalcitrant lignin structure. Nutrient content and ratio further influenced these outcomes, with manure-derived hydrochar promoting microbial biomass carbon (845 mg kg^{-1} vs. 350 mg kg^{-1} in control), while stalk-derived hydrochar was more effective at optimizing carbon sequestration. These findings highlighted the dual role of hydrochar in enhancing soil structure and SOC sequestration, with feedstock selection critically determining functional priorities. Such insights could provide valuable guidance for tailoring hydrochar production and application to improve agricultural sustainability through soil quality improvement.

*Correspondence:
Xiaoxuan Su
xuangood@swu.edu.cn
Ran Xiao
xiaoran0012@swu.edu.cn; xiaoran0012@gmail.com
Full list of author information is available at the end of the article

Springer

Highlights

- Hydrochars best enhanced soil aggregation and C sequestration in organic amendment trials.
- Hydrochars outperformed stalk and biochar in boosting soil structure and C storage.
- Mechanisms of hydrochar-induced soil aggregation and C sequestration were proposed.
- Stalk-derived hydrochar maximized soil aggregation and C sequestration over other feedstocks.
- DOC and TC in hydrochars are key mediators of soil structural and C storage changes.

Keywords Soil quality, Organic input, Hydrochar, Carbon-deficient cropland, Carbon fraction, Soil aggregates

Graphic Abstract

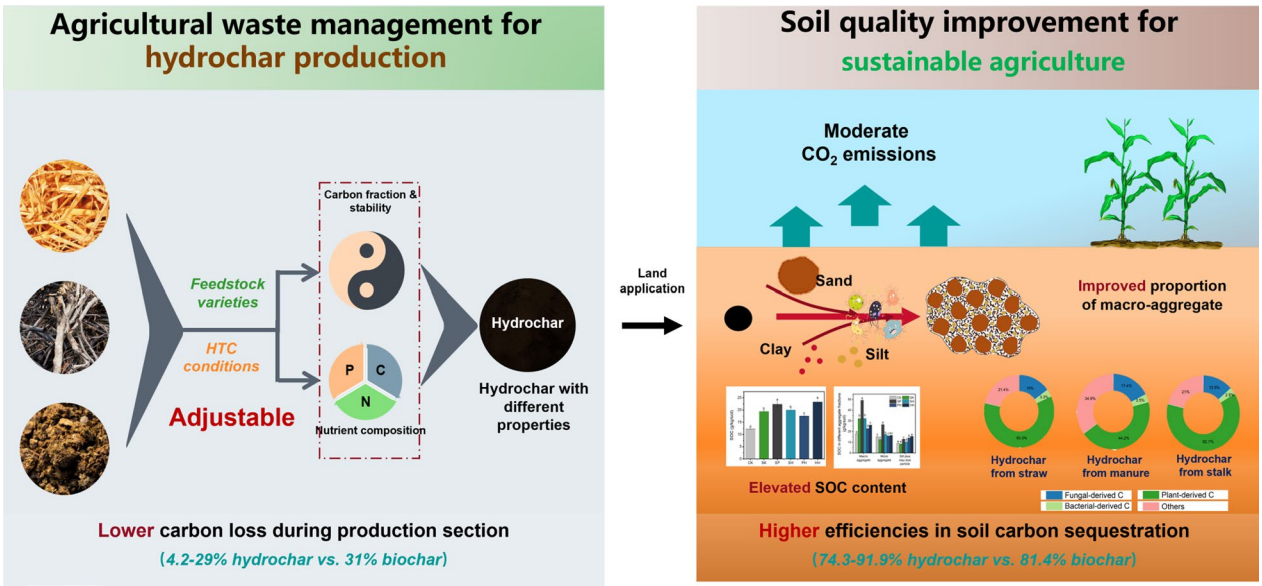

1 Introduction

Soils are the cornerstone of global food security, supporting over 94% of global food production (Lal et al. 2021; Richter 2021). As such, enhancing and preserving soil health has emerged as a central pillar of modern agricultural policy frameworks (Hu et al. 2020; Qiao et al. 2022). Soil organic carbon (SOC), a critical determinant of soil fertility, regulates crop productivity by stabilizing nutrient cycling and structural integrity (Beillouin et al. 2023; Li et al. 2024). According to Ma et al. (2023a, b), crop yields exhibit positive correlations with SOC content up to specific plateau thresholds, which are 43.2–43.9 g kg^{-1} for maize, 12.7–13.4 g kg^{-1} for wheat, and 31.2–32.4 g kg^{-1} for rice. However, the SOC levels in agricultural soils often fall below these optimal thresholds, exacerbating productivity constraints (Oldfield et al. 2019; Ma et al. 2024a). Meanwhile, soil aggregates, the structural units of soil, play a critical role in sustaining soil health, ecosystem sustainability, and agricultural yields (Ma et al. 2024b; Tian et al. 2022). For example, Cheng et al. (2023) found that improving soil structure through organic substitution and a concomitant decrease in sodicity favored sunflower growth (16–19% increase in plant height) and grain yield (8–9% improvement) in arid saline areas.

Exogenous organic amendments, such as natural organic residues (e.g., crop residue and livestock manure) and engineered materials (e.g., biochar and artificial humic substances), are critical for enhancing soil quality and function (Beillouin et al. 2023; Huang et al. 2024). Despite their recognized utility, their efficiencies in SOC formation and soil aggregation remain unsatisfactory (Wang et al. 2022; Ma et al. 2024b). For example, the efficiency of crop straws in SOC formation averages 20.5%, and that of livestock manure ranges from 19.1% to 27.9% (Li et al. 2023a; Ren et al. 2024). Biochar, though highly stable for long-term carbon sequestration, often fails to significantly enhance soil aggregation, particularly in

sandy soils, where its structural benefits remain constrained (UI Islam et al. 2021; Ma et al. 2024b). Collectively, these limitations highlight the urgent need for engineered amendments capable of synergistically improving both SOC stabilization and soil aggregate formation to address current agronomic inefficiencies.

Hydrochar, a carbon-rich solid material produced via hydrothermal carbonization (HTC) of wet organic biomass at temperatures between 180 and 260 °C, has recently emerged as a promising engineered amendment for solution for synergistically enhancing soil carbon sequestration and structural stability (Islam et al. 2021; Khosravi et al. 2022; Al-Nuaimy et al. 2024). Unlike conventional biochar, hydrochar uniquely integrates labile and recalcitrant carbon fractions (Kumar et al. 2020; Naisse et al. 2015), alongside abundant oxygen-containing functional groups (Fan et al. 2022). These intrinsic properties enable hydrochar to simultaneously expand soil carbon pools and improve aggregate stability (Bever and Coronella 2024; Rex et al. 2015; Wang et al. 2024a). For example, Yan et al. (2024) reported a striking 78–253% increase in SOC following hydrochar application (1%, w/w), outperforming unprocessed feedstocks by an order of magnitude. Furthermore, Heikkinen et al. (2019) and Tarf et al. (2022) found that hydrochars were more effective in promoting the formation of water-stable aggregates in soils compared to chars produced from slow pyrolysis or torrefied materials. Despite these advantages, field validation and mechanism exploration of hydrochar performance remain sparse. Influenced by feedstock and HTC processing parameters, the composition and properties of hydrochars show high variability (Bento et al. 2020; Xiong et al. 2024), further complicating their impacts of hydrochars on soil processes (Khosravi et al. 2022). For instance, Heikkinen et al. (2019) found that hydrochar efficacy in enhancing aggregate stability followed the sequence willow (HC-WW) > coffee cake (HTC-CC) > Scots pine bark (HTC-SPB) > brewery residue (HTC-BRE).

To address these knowledge gaps, we designed a microcosm incubation experiment to: (1) compare the dual efficiency of hydrochar in enhancing soil carbon sequestration and aggregate stability relative to natural (straw) and pyrolyzed (biochar) amendments; (2) evaluate feedstock-driven variability in hydrochar performance using different feedstocks for HTC, such as crop straw, livestock manure, and tree stalks; and (3) elucidate mechanisms linking hydrochar properties and soil carbon dynamics as well aggregation processes. We hypothesize that: (1) hydrochar will exhibit superior dual efficacy in expanding soil carbon pools and promoting aggregate formation relative to other organic amendments; (2) the performance of hydrochar depends greatly on its carbon fraction composition and physicochemical traits; and (3) the labile carbon fractions in hydrochars enhance aggregate formation and microbial-derived carbon accumulation, while recalcitrant fractions promote SOC persistence via chemical stability and physical protection within macroaggregates. We believe that the results of this study will broaden the hydrochar application in soil amendment and provide valuable guidance for tailoring hydrochar production and application to improve agricultural sustainability with enhanced soil health.

2 Materials and methods

2.1 Soils and organic amendments

Soil samples for this study were collected from a sorghum field in Jiangjing, Chongqing, China (106.219 E; 29.0429 N). The soils in this area are classified as purple soil (characterized by high calcium carbonate content and distinct red-to-purple coloration), which falls under the *Pup-Orthic Entisols* category in the Chinese taxonomy or *Regosols* in the FAO classification system. These soils are prevalent in the Sichuan Basin and are known for their moderate fertility and susceptibility to erosion, making them a critical focus for sustainable management strategies.

Prior to the sorghum-growing season, surface soil samples were randomly collected from five locations across the field using a stainless-steel shovel. The samples were thoroughly mixed to form a composite sample and transported to the laboratory promptly. After air-drying, the soil was ground and passed through a 2-mm sieve for subsequent incubation experiments. The basic physicochemical properties of the soil employed were as follows: pH 8.3 ± 0.08, SOC 14.1 ± 0.22 mg kg^{-1} soil, total N 0.87 ± 0.02 mg kg^{-1} soil, C/N 16.2, total P 0.455 ± 0.04 mg kg^{-1} soil, total K 19.0 ± 0.24 mg kg^{-1} soil, sand content 34.6%, clay content 35.6%, and silt content 29.8%.

Five types of organic amendments were used: maize straw (SK), biochar derived from maize straw (SP), hydrochar derived from maize straw (SH), pig manure (PH), hydrochar derived from Fagara (*Zanthoxylum bungeanum*) branch stalk (HH). SP was prepared by pyrolyzing maize straw at 550 °C for 2 h using a muffle furnace (Xiao et al. 2018). The hydrochars were prepared at 220 °C for 1 h using Teflon-lined autoclave reactors (50 ml). Detailed procedures regarding the preparation of hydrochar can be found in our previous works (Xiong et al. 2024). Selected properties of these amendments are summarized in Table 1. Before incubation, all organic amendments were oven-dried and subsequently ground to pass through a 0.25-mm sieve.

Table 1 The basic properties of organic amendments used in the presented study

Organic input	Total C (%)	Total N (%)	C/N	DOC (mg g^{-1})	Humic substance (%)	Humic acid (%)	Fluvic acid (%)	HA/FA
Maize straw (SK)	35.10 ± 1.74c	0.87 ± 0.20c	42.0	15.83 ± 0.65c	–	–	–	–
Maize straw biochar (SP)	49.80 ± 1.71a	0.76 ± 0.05c	65.5	4.04 ± 0.35d	–	–	–	–
Maize straw hydrochar (SH)	41.87 ± 2.26b	0.73 ± 0.13c	58.1	30.6 ± 2.30a	17.4 ± 0.44b	11.8 ± 0.78	5.63 ± 0.59b	2.11 ± 0.36
Pig manure hydrochar (PH)	25.50 ± 3.44d	1.99 ± 0.08a	12.8	28.1 ± 1.74a	15.3 ± 0.94b	9.72 ± 0.63	5.54 ± 0.83b	1.78 ± 0.32
Fagara stalk hydrochar (HH)	48.00 ± 1.34a	1.31 ± 0.07b	36.6	22.8 ± 1.27b	22.8 ± 1.45a	11.5 ± 0.90	8.30 ± 0.67a	1.75 ± 0.10

– means not analyzed

2.2 Microcosmic incubation experiment

To compare the effects of natural biomass, biochar, and hydrochar on soils and assess the performance differences among various hydrochars, two microcosm incubation experiments were conducted concurrently. These experiments were designed with quadruplicate treatments by mixing different organic amendments with soil at a rate of 2.5% (w/w) based on dry weight (Fig. 1). Specifically:

Experiment 1: included maize straw (SK), biochar derived from maize straw (SP), and hydrochar derived from maize straw (SH).

Experiment 2: included hydrochar from maize straw (SH), pig manure (PH), and hydrochar from Fagara (*Zanthoxylum bungeanum*) branch stalks.

Approximately 100 g of the soil-organic amendment mixture was transferred into 300-mL airtight glass jars. The soil moisture was adjusted to 60% of the water-holding capacity using deionized water. Each jar was sealed with Parafilm® perforated with several holes to allow air circulation, and incubated in darkness at 25 °C. Deionized water was added periodically to maintain consistent soil moisture content despite limited evaporation losses. A control treatment without organic inputs was also included for comparison. After 30 days of incubation, all samples were harvested destructively for further analysis. The duration of the incubation period was chosen based on previous studies (Watson et al. 2021; Wang et al. 2023a). Each soil sample was divided into three subsamples: (1) for analysis of microbial biomass carbon (MBC)

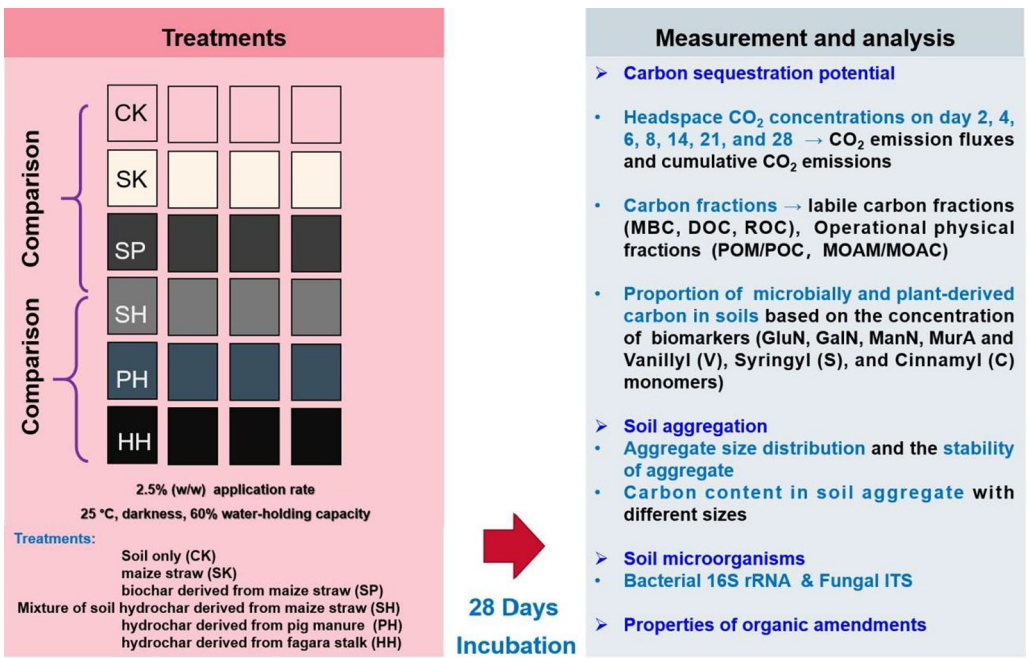

Fig. 1 Experimental setup and workflow of the microcosm incubation experiments with different organic amendments

and dissolved organic carbon (DOC), (2) for the assessment of major soil properties, including total nitrogen (TN), SOC and SOC fractions (i.e., particulate organic matter (POM) and mineral-associated organic matter (MAOM)), soil aggregate fractions, and contents of amino sugar and lignin phenol, and (3) for DNA extraction to analyze microbial communities.

Simultaneously, CO_2 emission fluxes and cumulative CO_2 emissions were quantified following the methods described in our previous study (Xiao et al. 2018). Briefly, 5 g of soil or soil-organic amendment mixture was placed into 50-mL borosilicate vials equipped with rubber septa and incubated at 25 °C for 30 days. Headspace CO_2 concentrations were measured on days 2, 4, 6, 8, 14, 21, and 28 using gas chromatography (Agilent 7890 B, Agilent Technologies Inc., USA) with a flame ionization detector (Model 3800, Varian Inc., Walnut Creek, CA, USA). After each sampling event, the vials were flushed with fresh air to continue the incubation process. CO_2 emission fluxes and cumulative CO_2 emissions were calculated using the following equations (Dong et al. 2023):

$$F = \rho \times \Delta C \times V \times 273/(273 + T) \times W \quad (1)$$

$$C = \sum_{i=1}^{n} (F_i + F_{i+1})/2 \times (t_{i+1} - t_i) \times 24 \quad (2)$$

where F is the CO_2 emission flux (mg kg^{-1} soil day^{-1}), ρ is the standard gas concentration of CO_2, ΔC is the difference in CO_2 levels between samples and the control after a certain incubation period, V is the volume of the incubation flask (mL), T is the incubation temperature (°C), W is the dry weight of the soil (kg), C is the cumulative CO_2 emission (mg kg^{-1}), ($t_{i+1} - t_i$) is the time interval between two adjacent measurements, and n is the total number of measurements.

2.3 Soil organic carbon and its aggregation distribution analysis

2.3.1 Determination of soil organic carbon and its fractionation

The SOC content was quantified using the $K_2Cr_2O_7$ oxidation-titration method as described by Liu et al. (2014), while the TN content was determined by dry combustion using an elemental analyzer (Vario EL iii, Elementar GmbH) (Chen et al. 2021). Microbial biomass carbon (MBC) was analyzed using the fumigation-extrication method (Bian et al. 2024). DOC was extracted by shaking soil samples with deionized water at a ratio of 1:10 (w/v) for 24 h, followed by filtration (<0.45 μm) and measurement with a Shimadzu TOC-VCPN analyzer (Shimadzu, Japan). Readily oxidizable carbon (ROC) was assessed using a 333 mmol L^{-1} $KMnO_4$ oxidation method (Chen et al. 2012). Furthermore, a 3-day incubation experiment was conducted to further evaluate the stability of SOC by measuring soil respiration rates and cumulative CO_2 emissions (Zhang et al. 2022).

For the persistence analysis of SOC, air-dried soil samples were separated into operational physical fractions, i.e., particulate organic matter (POM) fraction and mineral-associated organic matter (MAOM) fraction using 5 g L^{-1} sodium hexametaphosphate, following the methods described by Bian et al. (2024) and Yu et al. (2022). The carbon content in both fractions was determined using the $K_2Cr_2O_7$ oxidation-titration method. The relative contributions of POM-C (i.e., POC) or MAOM-C (i.e., MAOC) to total SOC were calculated as follows (Wang et al. 2023b):

$$R_{POC/MAOC} = (M_{POM/MAOM} \times C_{POM/MAOM})/SOC \quad (3)$$

where $M_{POM/MAOM}$ is the mass proportion of POM or MAOM, $C_{POM/MAOM}$ denotes the carbon content in each fraction, and $R_{POC/MAOC}$ indicates the relative contribution of POC or MAOC to total SOC, respectively.

2.3.2 Soil aggregate distribution and stability assessment

Soil aggregates were fractionated into three size classes: macroaggregates (2–0.25 mm), microaggregates (0.25–0.053 mm), and silt plus clay-size particles (<0.053 mm) through the wet-sieving method (Six et al. 1998). The separated fractions were subsequently oven-dried at 40 °C. Aggregate stability was evaluated by calculating the mean weight diameter (MWD) using the following formula (Liu et al. 2014):

$$MWD = \sum_{i=1}^{n} F_i \times D_i \quad (4)$$

where Fi is the mean diameter of aggregates remaining on the respective sieves (%), Di is the mean diameter of aggregates remaining on the respective sieves (mm), and n denotes the number of sieves used for aggregate separation.

The SOC content was also determined for all soil aggregate fractions, and the distribution of SOC at the aggregate scale was calculated as follows:

$$R_{aggregate\_i} = M_{aggregate\_i} \times C_{aggregate\_i}/SOC \quad (5)$$

where $M_{aggregate\_i}$ is the mass proportion of aggregate i, $C_{aggregate\_i}$ is the carbon content in aggregate i, and $R_{aggregate\_i}$ is the proportion of C in soils for aggregate i.

2.3.3 Amino sugars and lignin phenols analysis

2.3.3.1 Analysis of amino sugars Amino sugars in the soil were extracted and quantified using gas chromatography following the methods outlined by Bian et al. (2024). The concentrations of glucosamine (GluN), galactosamine (GalN), monoamine (ManN), and muramic acid (MurA) were measured and summed to represent the total amino sugar content. The fungal-derived and bacterial-derived C content was subsequently calculated using equations proposed by Liang et al. (2019):

$$\text{Fungal derived C} = (\text{GluN}/179.17 - 2 \times \text{MurA}/251.23) \times 179.17 \times 9 \quad (6)$$

$$\text{Bacterial derived C} = \text{MurA} \times 45 \quad (7)$$

where GluN and MurA are the quantities of GluN and MurA in soils (mg kg^{-1} soil), 179.2 and 251.2 are their respective molecular weights, and 9 and 45 are the conversion factors for inferring fungal-derived C and bacterial-derived C from GluN and MurA, respectively. The total microbial necromass carbon (MNC) was computed as the sum of fungal-derived C and bacterial-derived C.

2.3.3.2 Analysis of lignin phenols Soil lignin phenols were extracted and quantified using the copper oxide (CuO) oxidation method coupled with gas chromatography following the procedures described by Liao et al. (2024) and Bi et al. (2019). Lignin phenol content was determined by summing the concentration of Vanillyl (V), Syringyl (S), and Cinnamyl (C) monomers (Bian et al. 2024). The acid/aldehyde ratios for V and S phenols, denoted as ((Ad/Al)_v) and ((Ad/Al)_s), as well as the C/V and S/V ratios, were utilized to indicate the oxidation state and stability of plant substrates (Liao et al. 2024; Ma et al. 2023a). Plant-derived C in the total SOC was estimated using the following equation (Chen et al. 2021):

$$\text{P} = (\text{V}/33.3\% + \text{S}/90\% + \text{C})/(8\% \times \text{SOC}) \times 100\% \quad (8)$$

where V, S, and C denote the content of carbon in the V-, S-, and C-type phenols (g kg^{-1} soil), SOC represents the soil organic carbon content (g kg^{-1} soil), and 8% is the minimum of lignin content in the plant residues (Burgess et al. 2002).

2.3.4 DNA extraction and high-throughput sequencing analysis

Soil DNA extraction, PCR amplification, and Illumina sequencing were conducted by Shanghai Meiji Biomedical Technology Co., Ltd (Shanghai, China). Briefly, total DNA was extracted from soil samples using the E.Z.N.A® soil DNA Kit (Omega Bio-tek, Norcross, GA, USA) following the manufacturer's protocol. After determining the quality and concentration, primers 515F-806R and ITS1F-ITS2 were used for PCR amplification of the bacterial 16S rRNA (V3–V4 region) and fungal ITS1 region, respectively. The resulting PCR products were sequenced on an Illumina MiSeq PE300 system (Illumina Inc., San Diego, CA, USA) following the standard protocols at Biomarker Technologies Co., Ltd (Beijing, China).

The raw sequence reads were processed and analyzed using Quantitative insights into Microbial Ecology (QIIME) (version 1.9.1), including quality control and taxonomic assignment. Operational taxonomic units (OTUs) for bacteria and fungi were picked at 97% similarity using USEARCH (version 10.0) and clustered via UPARSE (version 7.0.1, Edgar 2013). Bacterial 16S rRNA sequences were aligned against the Silva database (v138), while fungal ITS sequences were matched to the UNITE database (v8.3).

2.4 Statistical analysis

Differences in CO_2 emissions, aggregate distribution, amino sugar content, and lignin phenol content were analyzed using one-way ANOVA with Duncan's post hoc test for multiple comparisons, using IBM SPSS Statistics 22, with the significant level set at $p < 0.05$. The beta diversity of both bacterial and fungal communities was assessed via principal coordinates analysis (PCoA), using Bray-Cutris dissimilarity matrices. Spearman rank correlations along with their associated p values among soil properties were visualized using Origin 2021. To further explore the relationships between soil properties (e.g., SOC, DOC, ROC, etc.) and the properties of organic inputs (e.g., C content, C/N ratio, and DOC), correlation analysis and Mantel tests were conducted using the "mantel" function in the "vegan" package of R.

3 Results

3.1 CO_2 emissions through the incubation period

As depicted in Fig. 2a, CO_2 emission fluxes exhibited a consistent temporal pattern across all treatments during the incubation period. Following a rapid increase, the fluxes peaked between days 2 and 4 and then gradually declined, stabilizing after day 15. Notably, the highest peak flux was observed for the HH and SK treatments, with peak values decreasing in the order of HH (310 mg kg^{-1} soil) > SK (261 mg kg^{-1} soil) > SH (226 mg kg^{-1} soil) > PH (208 mg kg^{-1} soil) > CK (27 mg kg^{-1} soil) and SP (15 mg kg^{-1} soil). Compared to SH and PH (~1500 mg CO_2 kg^{-1} soil) and CK (~250 mg CO_2 kg^{-1} soil), the cumulative CO_2 emissions

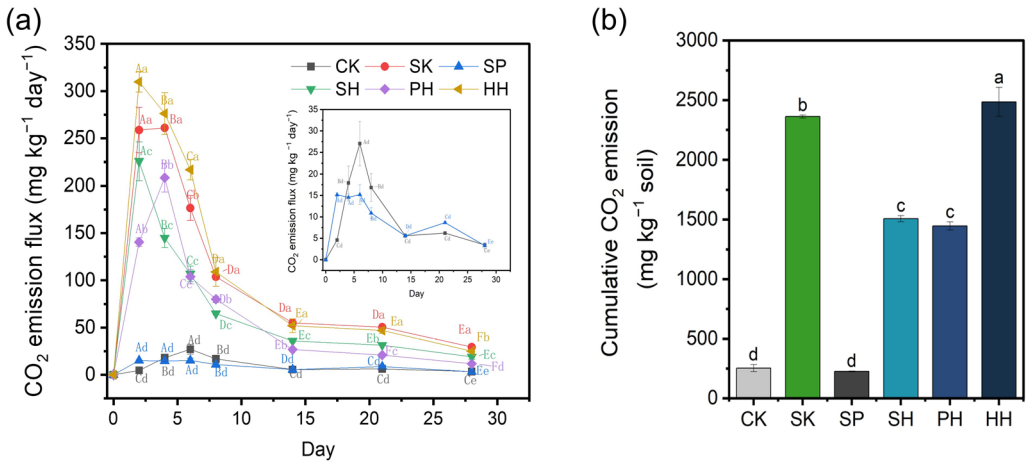

Fig. 2 Effect of different organic amendments on CO_2 emission flux and the cumulative CO_2 emission within the 28-day incubation experiment. **a** CO_2 emission flux and **b** cumulative CO_2 emission. CK: control, SK: maize straw, SP: straw-derived biochar, SH: straw-derived hydrochar, PH: pig manure-derived hydrochar, HH: stalk-derived hydrochar. The error bar is the standard deviation. Different letters represent significant differences among different treatments. Duncan's multiple-comparison test, $p < 0.05$

over the incubation period were significantly higher in HH and SK treatments (~2300 mg CO_2 kg^{-1} soil) ($p < 0.05$). In contrast, biochar amendment (SP) led to a moderate reduction in cumulative CO_2 emission (Fig. 2b). Considering the varying carbon contents of organic amendments (Table 1), carbon-normalized cumulative CO_2 emissions were calculated, which showed a ranked order of SK > PH > HH > SH > SP (Table S1).

3.2 Aggregate size distribution and aggregate stability

Changes in soil aggregate distribution and aggregate stability after incubation are illustrated in Fig. 3. Under the control treatment (CK), micro-aggregates dominated the soil aggregate, accounting for 42%, while macro-aggregates and silt plus clay-size fractions each comprised approximately 28% (Fig. 3a).

Except for biochar (SP), organic amendments increased the proportion of macro-aggregate to 56–71% compared to CK ($p < 0.05$). Among these, treatments with hydrochars (i.e., HH and PH) exhibited the most pronounced macroaggregate accumulation. Conversely, the proportions of micro-aggregates and silt plus clay-size fractions decreased upon application of crop straw (SK) and hydrochars (HH, PH, and SH) ($p < 0.05$). In contrast, biochar (SP) slightly decreased the proportion of micro-aggregate but significantly increased the proportion of silt plus clay-size particles in soils, suggesting a distinct mechanism compared to other organic amendments.

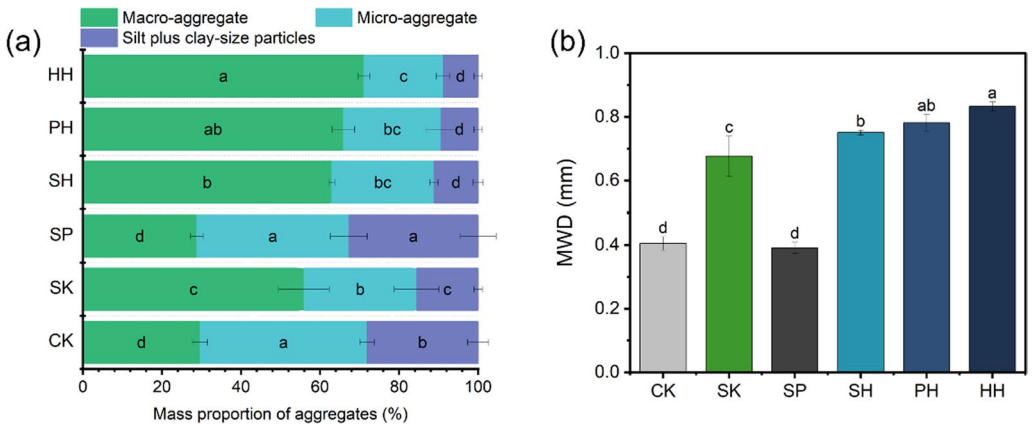

Fig. 3 Mass proportion of aggregates with different sizes (**a**) and the mean weight diameter (MWD) (**b**) among treatments with different organic amendments

Regarding aggregate stability, as indicated by MWD, the values decreased in the following order: HH ≈ PH (~0.80 mm) > SH (0.75 mm) > SK (0.68 mm) > CK and SP (~0.40 mm) (Fig. 3b).

3.3 SOC accumulation, fractions, and distribution across aggregate fractions

As expected, organic amendments significantly increased SOC content by 58–90% ($p < 0.05$), with the highest increments (~90%) observed in HH and SK, followed by SK, SH, and PH (43–63%) (Table 2). Notably, carbon efficiencies, calculated as the ratio of SOC increase to carbon inputs, were also the highest for HH (Table S1). This was followed by PH > SK > SP > SH, suggesting that hydrochar, particularly HH, demonstrated superior capacity to retain added C in soils. Additionally, cumulative net CO_2 emissions from soils were highest for SK (76.9 mg CO_2 kg^{-1} soil), followed by PH (56.4 mg CO_2 kg^{-1} soil), HH (51.5 mg CO_2 kg^{-1} soil), SH (37.2 mg CO_2 kg^{-1} soil), and SP (16.8 mg CO_2 kg^{-1} soil) (Fig. S1). All these indicated that hydrochars, despite their high C sequestration potential, may still undergo partial decomposition compared to biochar (SP), which exhibited exceptional stability.

Notably, the overall carbon efficiency was highest for hydrochars, particularly for those derived from lignocellulosic materials, as indicated by the relatively lower carbon losses during organic amendment preparation and the subsequent land application. As shown in Table S2, the overall carbon loss decreased in the order of SP (43.9%) > PH (41.3%) > SH (30.3%) > SK (18.5%) > HH (12.0%). The low carbon efficiency for SP was attributed to the substantial carbon loss during biochar production, accounting for over 75% of total carbon loss. In contrast, the relatively higher carbon efficiency for SK was mainly attributed to the short incubation period (30 days) in this study, as evidenced by the highest (Ad/Al) ratio among all treatments (Table S3), indicating strong degradation potential of lignin compounds.

Feedstock variability further shaped carbon efficiency. HH demonstrated the highest carbon efficiency with minimal carbon loss and higher carbon stability during hydrochar production and soil application, respectively. In contrast, manure-derived hydrochar enhanced soil fertility due to its abundant nutrient content, despite its moderate carbon efficiency (Table S4). Across treatments, organic amendments significantly elevated soil nitrogen and the C/N ratio compared to CK, with and increased available nutrients in soils: alkaline-N (by −4.9% to 49.4%), available P (by −1.6% to 72.1%), and potassium (by 3.5% to 144%) (Table S4).

SOC fractions exhibited marked differences among treatments (Table 2). Except for SP, all organic inputs significantly increased the contents of ROC, MBC, and DOC in soils relative to CK ($p < 0.05$), with the highest ROC, MBC, and DOC observed in SH (1.46 g kg^{-1} soil), PH (845 mg kg^{-1} soil) and SK (4516 mg kg^{-1} soil) treatments, respectively. Despite the notable SOC enrichment, the SH treatment resulted in lower MBC and DOC levels but a slightly higher ROC compared to other amendments. Particulate organic matter (POM) dominated the SOC pool, accounting for 79.6–83.4% of total SOC (Fig. 4a). Organic amendments further increased the proportion of POM, though the changes were not substantial. However, a significant increase in SOC content was observed in both POM (44–96%) and MAOM (20–59%) fractions with organic inputs ($p < 0.05$). Notably, the greatest increase in SOC within the POM fraction (i.e., POC) was observed for SP and HH, while the highest increase in SOC within the MAOM fraction (i.e., MOAC) occurred in HH (Fig. 4b, c). Overall, POC dominated, accounting for over 80% of the total SOC (Fig. 4d).

The distribution of SOC content across different aggregate size classes followed the order: macroaggregate > micro-aggregate > salt plus clay-size particle (Fig. 4e). Additionally, significant enhancement in SOC due to organic inputs predominantly occurred in macroaggregates, with increases ranging from 127% to 274% ($p < 0.05$). Specifically, the highest increase of SOC in

Table 2 Changes in the SOC content and its fractions among treatments with different organic amendments through incubation

Treatment	SOC (g kg^{-1} soil)	MBC (mg kg^{-1} soil)	DOC (mg kg^{-1} soil)	ROC (g kg^{-1} soil)	ROC/SOC (%)
CK	12.25 ± 0.16d	350 ± 44d	435 ± 17d	1.08 ± 0.22c	8.84 ± 1.69a
SK	19.40 ± 0.42b	782 ± 24b	4516 ± 398a	1.24 ± 0.06bc	6.39 ± 0.30b
SP	22.38 ± 1.10a	255 ± 11e	111 ± 8.0e	1.13 ± 0.03c	5.05 ± 0.13b
SH	20.03 ± 0.46b	765 ± 8.9b	567 ± 56c	1.46 ± 0.08a	7.29 ± 0.46ab
PH	17.56 ± 0.44c	845 ± 34a	3915 ± 145a	1.38 ± 0.20ab	7.89 ± 1.22ab
HH	23.28 ± 1.00a	622 ± 58c	861 ± 36b	1.19 ± 0.03bc	5.12 ± 0.12b

Different letters denote significant differences among treatments ($p < 0.05$, $n = 3$)

SOC soil organic carbon, *MBC* microbial biomass carbon, *DOC* dissolved organic carbon, *ROC* readily oxidizable carbon

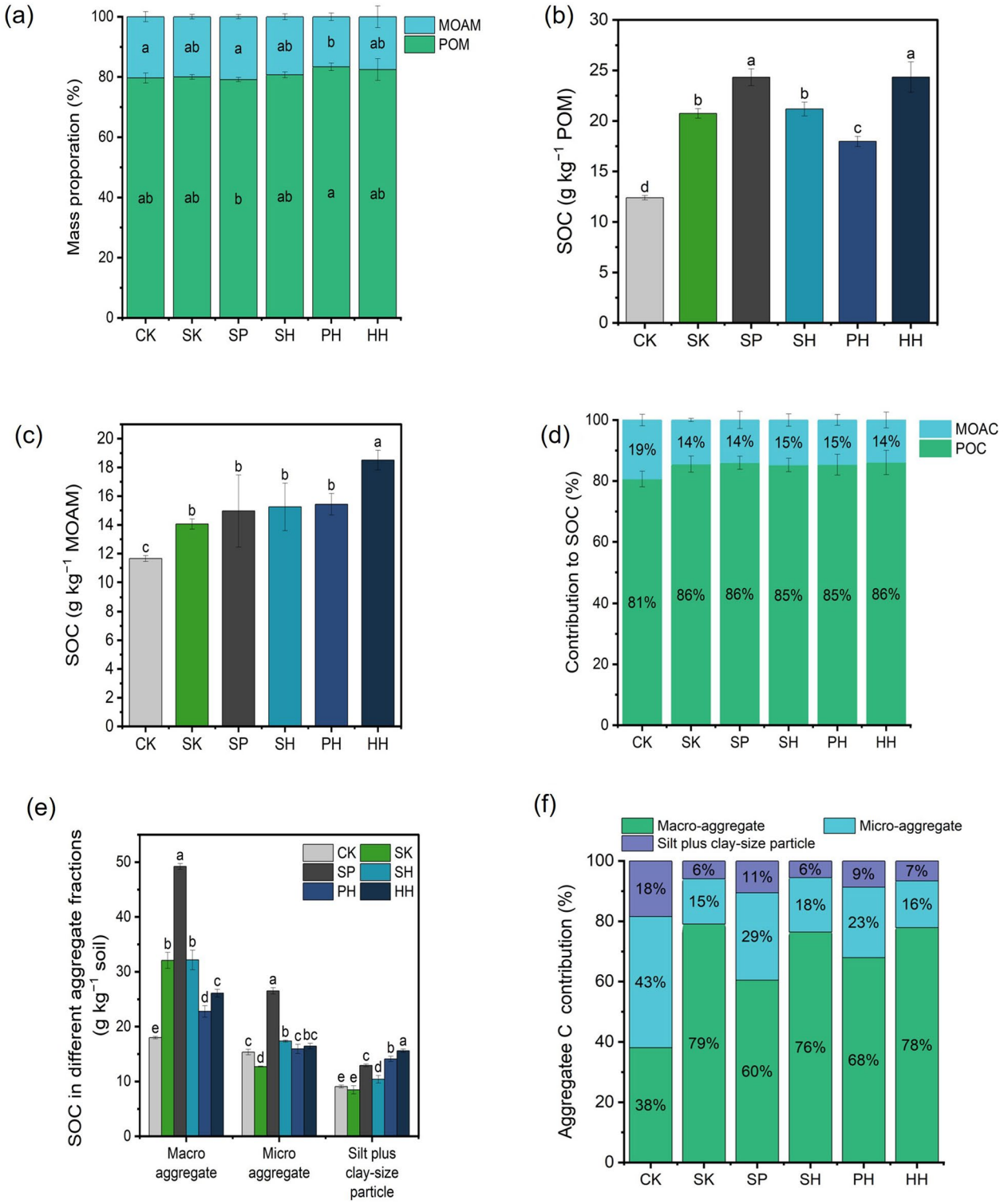

Fig. 4 Mass proportion of POM and MOAM in soils (**a**), SOC content in the POM fraction (**b**), MAOM fraction (**c**), and their contribution to the total SOC in soils (**d**), SOC content in different soil aggregate fractions (**e**) and the contribution of soil aggregate C to the total SOC in soils (**f**) among different treatments

the macro-aggregate was observed in the SP treatment. The straw treatment (SK) also significantly elevated SOC content in macro-aggregates, while it led to a decrease in micro-aggregates and silt plus clay-sized particles relative to CK. Hydrochar, regardless of the feedstock type, consistently increased SOC content across all three aggregate fractions compared to CK. Figure 4f highlights significant differences in the contribution of aggregate-C to the total SOC among treatments. In CK, the majority of carbon was accumulated in the micro-aggregate, followed by the macro-aggregate and silt plus clay-size fractions. Organic amendments substantially enhanced the contribution of macro-aggregate-associated C to the total SOC by 22–41%. Correspondingly, the contributions of micro-aggregate associated C and C in slit plus clay-size particles decreased with the application of organic amendments (Fig. 4f).

3.4 Amino sugar and lignin phenol accumulation in soils

Organic amendments, except for SP, significantly enhanced the content of amino sugars in soils ($p < 0.05$), with total amino sugar concentration ranging from 492 to 575 mg kg^{-1} soil (Fig. S2). Across treatments, GluN was the predominant amino sugar compound (308–375 mg kg^{-1} soil), followed by GlaN (158–173 mg kg^{-1} soil). In contrast, ManN and MurN exhibited much lower concentrations, both below 20 mg kg^{-1} soil. Notably, SK, PH, and HH applications led to a slight elevation in the GluN/MurN ratio by 4.5–7.3%, whereas SP exhibited a markedly lower GluN/MurN ratio compared to the other treatments (Table S3). In contrast to amino sugars, lignin phenol content demonstrated significant variation among treatments ($p < 0.05$) (Fig. S2). The highest lignin phenol concentrations were observed in SK, SH, and HH treatments, which increased by 245%, 236%, and 191%, respectively, compared to CK (533 mg kg^{-1} soil). Moreover, S-type phenols were most abundant in HH (52.3%), followed by V-type (38.2%) and C-type phenols (12.2%). In the other treatments, V-type and S-type phenols dominated (~35% each), with C-type phenols contributing less than 30% of the total lignin phenol content.

3.5 Microbial-derived and plant-derived C and its contributions to SOC

The concentration of microbial-derived C varied among treatments, following the order: HH > SK > PH > SP > CK > SP, with values ranging from 3.237 to 3.852 g kg^{-1} soil. Fungal-derived C was the main contributor, accounting for over 80% of the microbial-derived C in soils (Fig. 5a). In contrast, plant-derived carbon ranged from 5.90 to 14.96 g kg^{-1} soil, with the greatest concentration observed in the SK, SH, and HH treatments (Fig. 5b).

The contributions of carbon from different sources to SOC were further examined, as illustrated in Fig. 5c–h. In CK, plant-derived C accounted for more than 50% of SOC, followed by fungal-derived C (22%) and bacterial-derived C (20%). The application of organic amendments significantly altered the proportions of carbon from different sources within total SOC, with distinct variations observed among treatments. For instance, straw application (SK) increased the proportion of plant-derived C by 20%, while biochar application (SP) markedly enhanced the contribution of C from other sources. Interestingly, the impacts of hydrochar on SOC composition varied significantly depending on the feedstock. Specifically, SH and HH treatments notably increased the proportion of plant-derived C, while PH treatment substantially elevated the proportion of carbon from other sources.

3.6 Soil microbial community composition

Changes in bacterial community composition are depicted in Fig. S3. Although no significant differences were observed in the alpha diversity of the bacterial community, treatments with organic amendments exhibited reduced richness and diversity of colonies (Fig. S3a, b). The high number of unique ASVs shown in the Venn diagram (Fig. S3c) and the PCoA diagram (Fig. S3d) indicated substantial differences in bacterial communities among treatments. Specifically, the dispersion of bacterial communities between CK/SP and other treatments suggested that hydrochar and straw applications had a pronounced impact on soil bacterial communities. *Actinobacteriota* and *Proteobacteria* were the dominant bacterial phyla, accounting for 28.5–39.2% and 26.1–31.1% of the total bacterial phyla in soils, respectively. Compared to CK and SP, hydrochar and straw applications increased the proportion of *Actinobacteriota* and *Firmicutes*, while reducing that of *Chloroflexi*, *Acidobacteriota*, and *Myxococcota* (Fig. S3e). At the genus level, organic amendments enhanced the proportion of *Bacillus* and *Streptomyces* in soils, particularly in HH treatments (Fig. S3f). Furthermore, a co-occurrence correlation network was constructed to identify key bacteria and explore relationships within bacterial communities (Fig. S3g). More developed bacterial co-occurrence networks were observed in SP and SK, with no apparent differences in nodes and edges between SK and the hydrochar treatments (Table S5). Additionally, the majority of the notes belonged to *Actinobacteriota*, *Proteobacteria*, *Firmicutes*, and *Bacteroidota*.

Similarly, organic amendments slightly decreased the richness and diversity of fungal colonies, particularly noticeable in SP and PH treatments (Fig. S4).

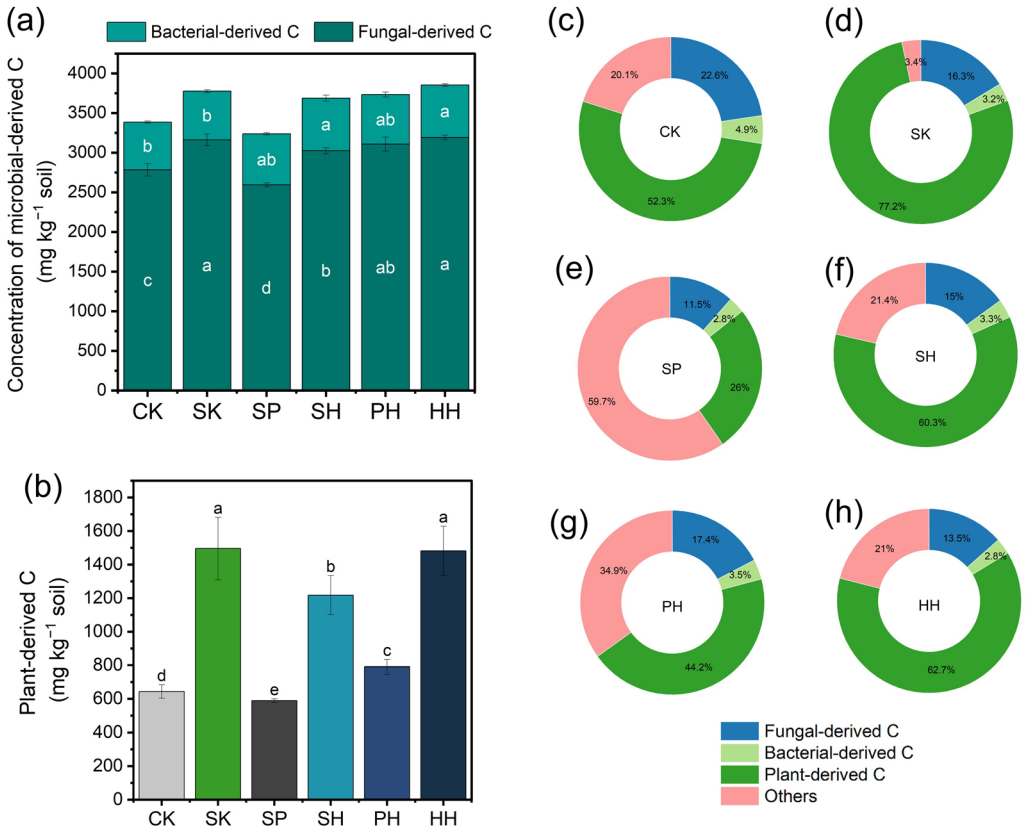

Fig. 5 The concentration of microbe-derived C (**a**), and plant-derived C (**b**) in soils among different treatments, and the contribution of carbon from various sources (i.e., plant, bacterial, fungal, and others) to total SOC in soils for CK (**c**), SK (**d**), SP (**e**), SH (**f**), PH (**g**), and HH (**h**)

Significant differences in fungal community composition were also observed, as indicated by the Venn diagram and PCoA analysis results (Fig. S4c, d). Interestingly, samples from CK, SK, and SP clustered together, indicating high similarity in their fungal communities. Across all treatments, *Ascomycota* was the most abundant fungal phylum, ranging from 73.3 to 91.7% (Fig. S4e). On the genus level, CK and SP showed high similarity with *Aspsergillus* and *Talaromyces* as dominant genera (Fig. S4f). In contrast, SH and SK treatments significantly reduced the abundance of *Aspsergillus* and *Talaromyces*, while greatly increasing the abundance of *Schizothecium*. Moreover, the proportion of *Neocosmpospora*, *Gibberella*, and *Chaetomium* greatly increased in PH, and the proportion of *Aspergillus*, *Chaetomium*, and *Neocosmospora* increased in HH compared with CK (Fig. S4f). Similar to bacteria, more developed fungal co-occurrence networks were observed in SP treatments (Fig. S4g). Moreover, treatments with organic inputs exhibited higher nodes, edges, and average degrees compared to CK, indicating enhanced interactions among fungal communities (Table S5).

3.7 Correlations among characteristics of organic inputs and soil microorganisms on soil aggregation and SOC accumulation, and fractionation

The Spearman correlation analysis revealed significant correlations among the characteristics of organic inputs, soil microorganisms, and their effects on soil aggregates and SOC accumulation and fractionation (Fig. 6). Specifically, MWD was positively correlated with labile forms of SOC (i.e., MBC and ROC), cumulative CO_2 emissions, MAOC, amino sugar content, lignin phenol content, and fungi richness, while it exhibited negative correlations with carbon in micro-aggregates, bacterial richness, and bacterial diversity ($p < 0.05$). Additionally, SOC and ΔSOC were positively correlated with soil TN, the soil C/N ratio, and the carbon content of various fractions, but negatively correlated with bacterial richness ($p < 0.05$).

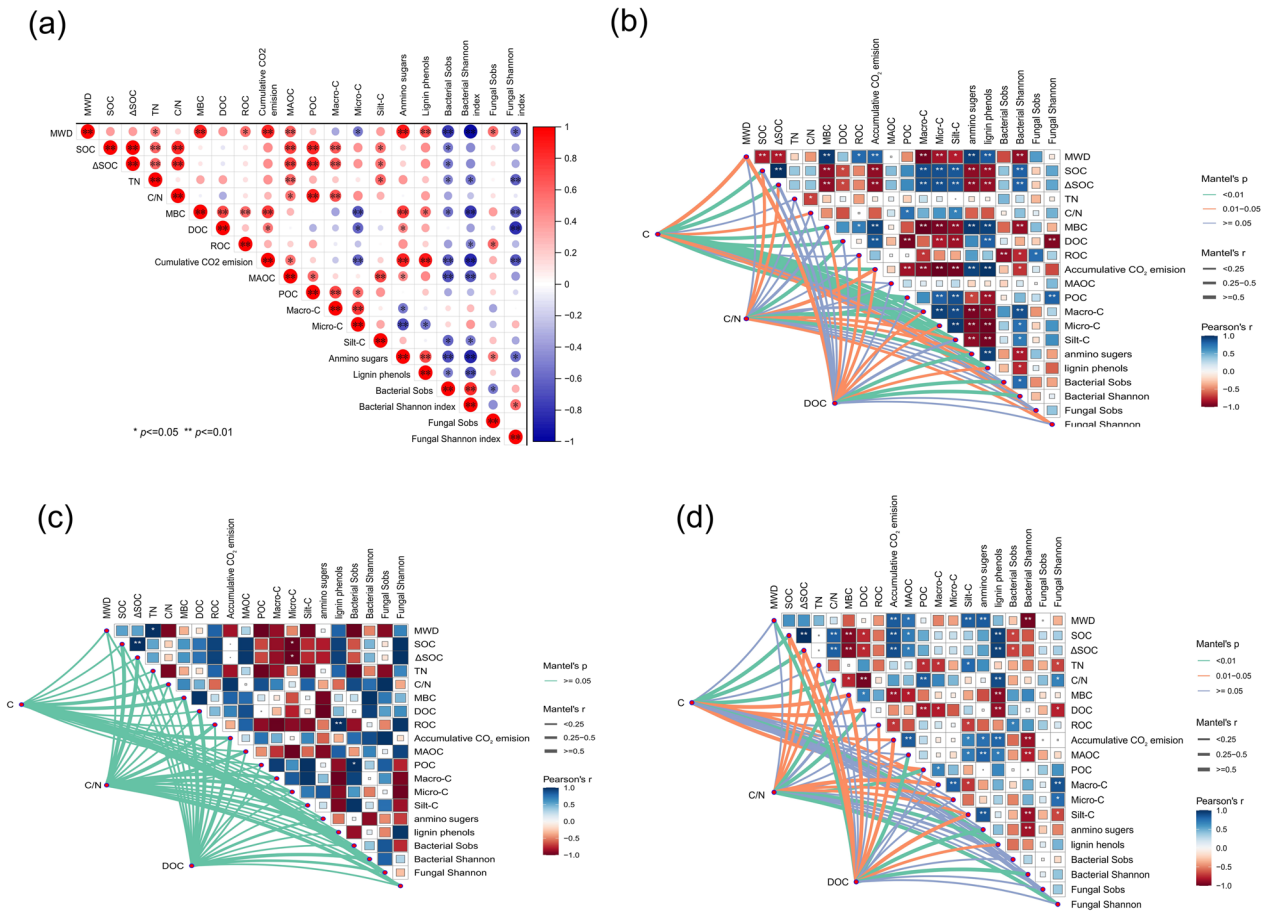

Fig. 6 Spearman correlation heatmap showing the correlation between SOC/soil aggregation and typical soil properties (**a**); Pearson's correlation (*r*) mantel-test heatmap of the carbon content, C/N ratio, and DOC content with several soil properties such as SOC content and fraction, aggregate stability, and microbial abundance and diversities for straw (**b**), biochar (**c**), and hydrochars produced from different feedstocks (**d**). The colors indicate pairwise comparisons of variables, and the thicknesses of the lines indicate the strength of the correlation. The asterisks indicate the statistical significance. * $p < 0.05$; ** $p < 0.01$. C, C/N, and DOC represent the carbon content, C/N ratio, and DOC content of different organic materials, respectively. ΔSOC represents the increase in SOC compared to the control. Macro-C, Micro-C, and Silt-C represent the SOC content in macro-aggregates, micro-aggregates, and silt and clay particles, respectively

The Pearson correlation (*r*) Mantel-test heatmap (Fig. 6b–d) highlighted significant variations in the correlations between the typical properties of organic amendments and soil characteristics. Specifically, the C content of straw exhibited a highly significant positive correlation with SOC, ΔSOC, MBC, DOC, cumulative CO_2 emissions, POC, and C in different aggregate fractions, amino sugar content, and lignin phenol content ($p < 0.01$). Moreover, both the DOC and lignin phenol content showed a significant positive correlation with the C/N ratio of straw ($p < 0.01$). The impact of straw-derived DOC was primarily reflected in its influence on soil bacteria ($p < 0.01$), followed by MWD, MBC, ROC, cumulative CO_2 emissions, and C in macro-aggregates ($p > 0.05$). Notably, while biochar properties were positively correlated with soil properties, these relationships were not particularly strong ($p > 0.05$). For hydrochars, the carbon content demonstrated a highly significant positive correlation with SOC, ΔSOC, C/N ratio, and lignin phenols content ($p < 0.01$). Additionally, the C/N ratio of hydrochars was significantly and positively correlated with the the soil C/N ratio, DOC, POC, lignin phenol content, and the diversity of fungi ($p < 0.01$). Furthermore, hydrochar-derived DOC was positively correlated with MWD, amino sugar content, and bacterial diversity ($p < 0.01$).

4 Discussion

4.1 Organic input-induced soil aggregation and aggregate stabilization

Soil aggregates are clusters of soil particles that adhere more strongly to one another than to adjacent particles. Enhancing aggregate stability is vital for maintaining soil structure, influencing aeration, water infiltration and retention, nutrient cycling, carbon sequestration, and

root penetration and growth (Ma et al. 2024b; Tian et al. 2022). Studies have shown that the organic amendments can improve soil aggregation either directly by providing organic "glue" agents (e.g., polysaccharides, humic substances, and other sticky extracellular materials) and inorganic binding units (e.g., cations like Ca^{2+} and Mg^{2+}) (Amelung et al. 2023; Sonsri and Watanabe 2023) or indirectly by fostering soil microorganisms through the mediation of the micro-environment and the supply of labile organic substrates (Angulo et al. 2024; Sun et al. 2020). For these reasons, enhanced soil aggregation among treatments with organic inputs was observed in the present study (Fig. 3).

Compared to other amendments, hydrochars, regardless of feedstocks, showed higher efficiencies in enhancing soil aggregation with a dramatic increase in the proportion of macro-aggregate (112–140%) and MWD (85–106%) (Fig. 3). This may be attributed to their labile carbon compounds as well as to induced changes in soil microorganisms (Table 1; Fig. 6d; Figs. S3 and S4). For example, Song et al. (2022) and Sonsri and Watanabe (2023) found that increases in soil macro-aggregate were closely related to dissolved organic matter (DOM), specifically polysaccharides and N-containing compounds in soil amendments. They also confirmed that a higher abundance of high-molecular-weight DOM further enhanced soil aggregation by contributing to aggregate formation (Sonsri and Watanabe 2023). Apart from exogenous carbon, the relatively higher abundance of *Actinomycete* in bacterial communities and *Aspergillus* in fungal communities partly explained the enhanced soil aggregation observed in treatments with hydrochars, due to their high ability to facilitate aggregation (Rashid et al. 2016; Zhao et al. 2024) (Figs. S1 and S2). However, George et al. (2012) argued that hydrochar-induced soil aggregation mainly resulted from organic matter provision rather than cooperation between hydrochar, plants, and Arbuscular mycorrhiza. This is because the enrichment of organic compounds such as polycyclic aromatic hydrocarbons and phenols through HTC has been reported to be toxic to soil microorganisms (Andert and Mumme 2015; Si et al. 2024). Despite that, the response of soil microorganisms to hydrochars varied greatly depending on their physicochemical properties and compositions (Yan et al. 2024; Xiong et al. 2024, 2025). Differences in the physicochemical properties (i.e., humification degree, carbon content, and stability) and composition (i.e., compounds and molecular weight) of both extractable and non-extractable fractions in hydrochars may also account for the varied responses of soil aggregate to hydrochars (Ma et al. 2024b; Song et al. 2020; Wang et al. 2024b) (Fig. 2). However, empirical investigations into these mechanisms remain scarce to date. Future research should prioritize disentangling the direct and indirect effects of hydrochar application on soil aggregate stability, thereby advancing our mechanistic understanding of their roles in soil structural dynamics.

In contrast to prior findings (Ma et al. 2024b), biochar application exhibited limited effects on soil aggregation in this study, which can be explained by the alkaline soil pH (8.3), sandy soil texture, and lower DOC content in biochar, which collectively constrain aggregate formation (Ul Islam et al. 2021). Additionally, reduced microbial biomass carbon (MBC) levels (Table 2) further hindered the microbial-driven processes critical to aggregate stability, consistent with earlier reports (Sun et al. 2021).

4.2 Exogenous organic inputs induced soil carbon accumulation and fraction distribution

The accumulation of SOC arises from a dynamic balance between carbon inputs and outputs, involving processes such as the decomposition and stabilization of exogenous organic inputs and the decomposition of indigenous SOC (Mustafa et al. 2020). During this process, chemical recalcitrance of organic inputs, physical protection within macro-aggregate, and chemical stabilization via organo-mineral associations are key mechanisms that facilitate carbon sequestration (Cotrufo et al. 2019; Even and Cotrufo 2024; Lehmann and Kleber 2015).

As shown in Fig. 2, higher carbon content in organic amendments, particularly labile carbon, leads to a great initial CO_2 emission, which gradually declines over time as labile substrates are depleted (Xiao et al. 2018). Concurrently, exogenous inputs trigger microbial community shifts that accelerate native SOC decomposition (Huo et al. 2022), contributing to the emissions quantified in Fig. 2b.

Consistent with previous studies (Ma et al. 2024b; Zhang et al. 2024), organic inputs universally increased SOC levels across all aggregate size fractions (Fig. 4f). However, the magnitude of SOC accumulation differed among fractions, primarily due to differences in the composition, stability, and carbon content of organic inputs (Ma et al. 2024b; Verrone et al. 2024) (Table 1). Noticeably, macro-aggregates exhibited the most pronounced carbon enrichment (Fig. 4b), consistent with the aggregate hierarchy model (Li et al. 2023b; Six et al. 2004), where macroaggregates serve as primary storage pools for exogenous carbon. In contrast, the smaller increase in SOC content in micro-aggregates and silt plus clay-size particles was primarily driven by microbial processing and decay products via ex-vivo pathways (Krause et al. 2019).

Partitioning SOM into POM and MAOM is helpful for clarifying the dynamics of SOC, as these fractions differ in the biochemical properties and turnover rates

(Yu et al. 2022). According to Lavallee et al. (2020), fresh plant inputs can either be incorporated into POM via fragmentation or transition to MAOM through microbial modifications. As shown in Fig. 4, increases in SOC stocks were predominantly in the POM fraction, reflecting its sensitivity to exogenous carbon (Bian et al. 2024). Specifically, HH and SP outperformed other inputs in boosting POC, attributed to their high carbon content and stability (Bian et al. 2024). Additionally, the substantial increase in MOAC with stalk hydrochar application (HH) may stem from labile carbon influx (Table 1) and microbial community shifts (Sokol et al. 2019). Similarly, Cotrufo et al. (2022) found that soluble plant compounds boost MAOM formation, while structural compounds and microbial interactions favor POM. In addition, soil texture, particularly clay content, could also modulate POM/MAOM responses to amendments (Jilling et al. 2020). Although POM is generally considered less stable and has a shorter residence time compared to MAOM, significant increases in POM from highly recalcitrant organic inputs such as biochar and hydrochar may alter POM dynamics, warranting further investigation.

Exogenous inputs, especially recalcitrant ones (Table S5), shift SOC source contributions (Fig. 5c–h). While plants and microbes traditionally dominate SOC in ecosystems, Chen et al. (2024a, b) observed reduced proportional contributions from these sources (down 24.2–30.0% for plant-derived and 16.4–56.9% for microbial-derived C with biochar) due to residual input accumulation. Notably, the high proportion of plant-derived C in treatments with hydrochars was due to the incomplete degradation of lignocellulose through HTC (Khan et al. 2019). Collectively, differences in carbon loss, aggregate distribution, and input stability generate distinct SOC accumulation patterns across treatments.

4.3 Hydrochar-induced soil aggregation and SOC accumulation

Based on our analysis, the impacts of hydrochars on soil aggregation and SOC sequestration can be encapsulated in a conceptual framework (Fig. 7). Hydrochars produced under moderate hydrothermal conditions possess a dual-component architecture: (1) labile organic fractions composed of low-molecular-weight compounds and (2) recalcitrant carbon skeletons derived from partially degraded lignocellulosic residues. These structural characteristics confer hydrochars with unique abilities to synergistically influence soil structure and carbon cycling pathways.

Labile organic compounds play a crucial role in enhancing soil aggregation, either directly by providing organic binding agents or indirectly by modulating soil microbial communities. Conversely, the stable carbon skeleton is predominantly enriched in POM through fragmentation processes. Some labile organic compounds bind to clay particles via adsorption or through microbial ex vivo modifications, contributing to MAOM. Moreover, portions of the stable structural skeletons may be incorporated into MAOM via microbial in vivo turnover. The input of labile carbon and nutrients (e.g., nitrogen and phosphorus) stimulates microbial activity, thereby increasing the proportion of microbially derived carbon within the total SOC pool. Notably, due to incomplete degradation of lignocellulosic biomass during hydrothermal carbonization, plant-derived carbon also increases following the application of hydrochar. Consequently, SOC pools are composed of contributions from plant-derived, microbially derived, and hydrochar-originated carbon. In summary, the role of hydrochar in SOC accumulation is determined by a combination of physical and chemical properties, as well as the stability and molecular complexity of the feedstock.

5 Research limitations

This study provides significant insights into the dual efficacy of hydrochar in enhancing soil organic carbon (SOC) and improving soil aggregation. However, several limitations need to be acknowledged: Firstly, the short-term microcosm incubation period of 28 days may not adequately capture long-term SOC persistence, aggregate stability, or microbial community shifts. Soil processes such as carbon mineralization, aggregate turnover, and microbial necromass accumulation often require extended periods (e.g., >60–90 days) to stabilize. (Dong et al. 2023). Secondly, the absence of isotopic tracing (e.g., ^{13}C-labled substrates) limits our ability to distinguish exogenous carbon contributions from native SOC (e.g., priming effects) or disentangle the role of labile and recalcitrant carbon fraction of hydrochar on SOC formation as well as the fraction of SOC. Although biomarker analysis (i.e., amino sugar and lignin phenols) revealed the impacts of hydrochar on the divergent accumulation of microbial necromass and plant lignin components during incubation, this limitation remains (Ma et al. 2018). Thirdly, the lack of field validation restricts the practical relevance of the findings. Microcosm conditions cannot fully replicate field-scale complexities such as climate variability, crop interactions, or tillage disturbances. Furthermore, economic and scalability considerations—such as hydrochar production costs, energy inputs, and feedstock availability—were not evaluated, yet these factors are critical for assessing real-world feasibility. Therefore,

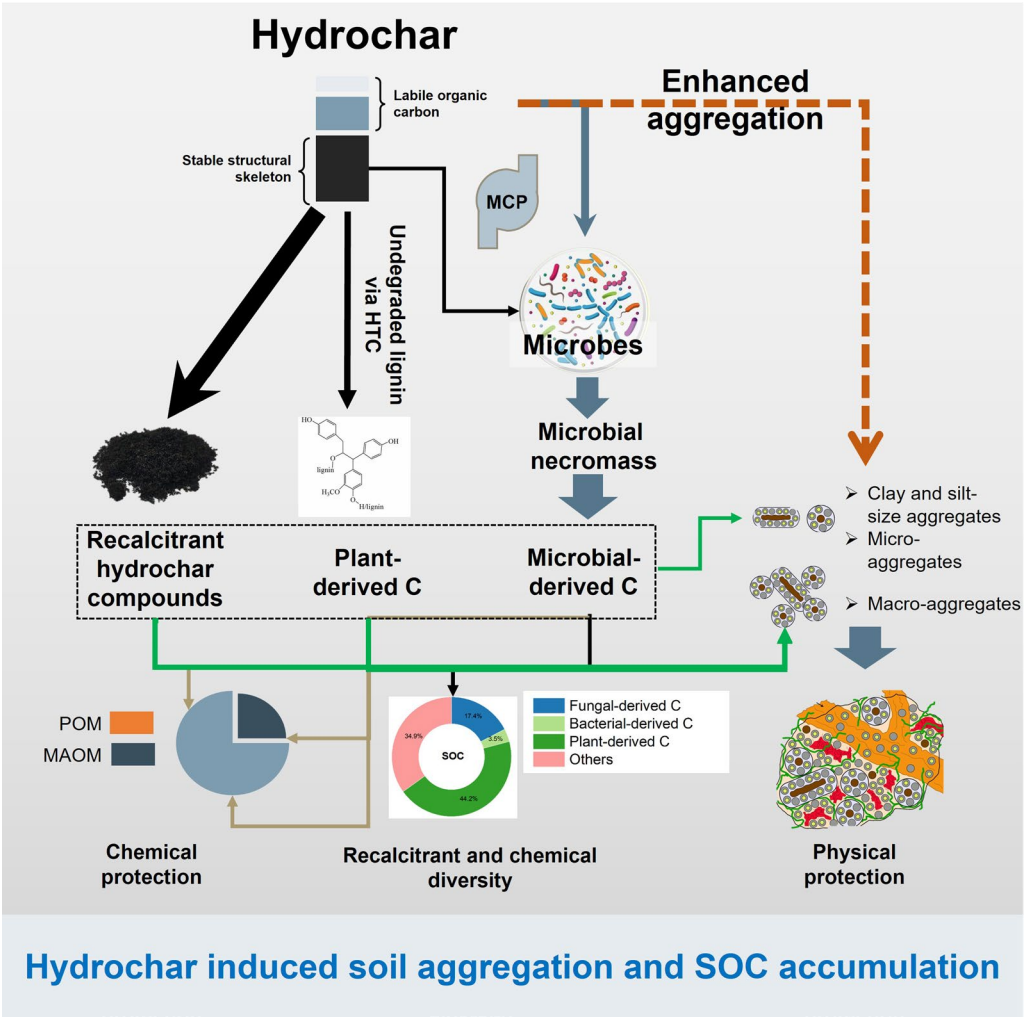

Fig. 7 Schematic paragraph showing hydrochar-induced soil aggregation and SOC accumulation

future studies should incorporate longer-term experiments, isotopic tracing, multi-soil validations, and field trials to address these gaps and inform scalable strategies for hydrochar deployment.

6 Conclusion

This study underscored the remarkable dual capacity of hydrochar to enhance SOC sequestration and soil aggregation, surpassing the performance of biochar and straw. Nonetheless, the efficacy of hydrochar varied significantly depending on its feedstock, due to differences in organic composition, stability, and nutrient content. Importantly, future research should focus on the long-term impacts of hydrochar on soil quality. Additionally, efforts should be directed towards optimizing hydrochar performance by elucidating the underlying mechanisms that govern its behavior in soil systems.

Supplementary Information

The online version contains supplementary material available at https://doi.org/10.1007/s42773-025-00547-y.

Additional file 1.

Author contributions

Liyang Sun: Methodology; Data curation; Investigation; Writing–original draft preparation; Software. Wei Sun, Pingping Ye: Formal analysis; Investigation. Yue Deng, Xiangtian Meng, Validation; Data curation. Ronghua Li, Zongsheng Zhang, Jim J. Wang: Writing- Reviewing and Editing. Xiaoxuan Su, Ran, Xiao: Conceptualization; Funding acquisition, Supervision; Validation; Visualization; Writing-Reviewing and Editing. The author(s) read and approved the final manuscript.

Funding
This work is funded by the Key Technologies Research and Development Program of China (2022YFD1901402), Key Research and Development Project for Tibet Autonomous Region (No. XZ202501ZY0056; XZ202201ZY0003N), and Chongqing Municipal Environmental Protection Bureau (2023-003/002).

Declarations

Competing interests
Jim J. Wang is an EBM of the journal Biochar, and he was not involved in the peer-review or handling of the manuscript. The authors declare that they have no known competing financial interests or personal relationships that could have appeared to influence the work reported in this paper.

Author details
[1]Interdisciplinary Research Center for Agriculture Green Development in Yangtze River Basin, College of Resources and Environment, Southwest University, Beibei, Chongqing 400715, People's Republic of China. [2]School of Plant, Environment and Soil Sciences, Louisiana State University Agricultural Center, Banton Rouge, LA 70803, USA. [3]Key Laboratory of Ecosystem Network Observation and Modeling, Institute of Geographic Sciences and National Resources Research, Chinese Academy of Sciences, Beijing 100101, People's Republic of China. [4]College of Natural Resources and Environment, Northwest A&F University, Yangling 712100, Shaanxi, People's Republic of China. [5]State Key Laboratory of Black Soils Conservation and Utilization, Institute of Northeast Geography and Agroecology, Chinese Academy of Sciences, Changchun 130012, Jilin, People's Republic of China.

Received: 5 November 2024 Revised: 8 June 2025 Accepted: 6 November 2025
Published online: 04 March 2026

References

Al-Nuaimy MNM, Azizi N, Nural Y, Yabalak E (2024) Recent advances in environmental and agricultural applications of hydrochars: a review. Environ Res 250:117923. https://doi.org/10.1016/j.envres.2023.117923
Amelung W, Meyer N, Rodionov A, Knief C, Aehnelt M, Bauke SL, Biesgen D, Dultz S, Guggenberger G, Jaber M, Klumpp E, Kögel-Knabner I, Nischwitz V, Schweizer SA, Wu B, Totsche KU, Lehndorf E (2023) Process sequence of soil aggregate formation disentangled through multi-isotope labelling. Geoderma 429:116226. https://doi.org/10.1016/j.geoderma.2022.116226
Andert J, Mumme J (2015) Impact of pyrolysis and hydrothermal biochar on gas-emitting activity of soil microorganisms and bacterial and archaeal community composition. Appl Soil Ecol 96:225–239. https://doi.org/10.1016/j.apsoil.2015.08.019
Angulo V, Bleichrodt RJ, Dijksterhuis J, Erktan A, Hefting MM, Kraak B, Kowalchuk GA (2024) Enhancement of soil aggregation and physical properties through fungal amendments under varying moisture conditions. Environ Microbiol 26(5):e16627. https://doi.org/10.1111/1462-2920.16627
Beillouin D, Corbeels M, Demenois J, Berre D, Boyer A, Fallot A, Feder F, Cardinael R (2023) A global meta-analysis of soil organic carbon in the Anthropocene. Nat Commun 14(1):3700. https://doi.org/10.1038/s41467-023-39338-z
Bento LR, Melo CA, Ferreira OP, Moreira AB, Mounier S, Piccolo A, Spaccini R, Bisinoti MC (2020) Humic extracts of hydrochar and Amazonian Dark Earth: molecular characteristics and effects on maize seed germination. Sci Total Environ 708:135000. https://doi.org/10.1016/j.scitotenv.2019.135000
Bever CG, Coronella CJ (2024) Carbon sequestration potential of manure-derived hydrochar aided by secondary stabilization. ACS Sustainable Chem Eng 12(14):5705–5715. https://doi.org/10.1021/acssuschemeng.4c00857
Bi WY, Wang JJ, Dodla SK, Gaston LA, DeLaune RD (2019) Lignin chemistry of wetland soil profiles in two contrasting basins of the Louisiana Gulf coast. Org Geochem 137:103902. https://doi.org/10.1016/j.orggeochem.2019.103902
Bian Q, Zhao LX, Cheng K, Jiang YJ, Li DM, Xie ZB, Sun B, Wang XY (2024) Divergent accumulation of microbe- and plant-derived carbon in different soil organic matter fractions in paddy soils under long-term organic amendments. Agric Ecosyst Environ 366:108934. https://doi.org/10.1016/j.agee.2024.108934
Burgess MS, Mehuys GR, Madramootoo CA (2002) Decomposition of grain-corn residues (*Zea mays* L.): a litterbag study under three tillage systems. Can J Soil Sci 82(2):127–138. https://doi.org/10.4141/s01-013
Chen XM, Liu JX, Deng Q, Yan JH, Zhang DQ (2012) Effects of elevated CO_2 and nitrogen addition on soil organic carbon fractions in a subtropical forest. Plant Soil 357(1–2):25–34. https://doi.org/10.1007/s11104-012-1145-3
Chen XB, Hu YJ, Xia YH, Zheng SM, Ma C, Rui YC, He HB, Huang DY, Zhang ZH, Ge TD, Wu JS, Guggenberger G, Kuzyakov Y, Su YR (2021) Contrasting pathways of carbon sequestration in paddy and upland soils. Glob Change Biol 27(11):2478–2490. https://doi.org/10.1111/gcb.15595
Chen Y, Zwieten LV, Xiao K, Liang C, Ren J, Zhang A, Li Y, Dong H, Sun K (2024a) Biochar as a green solution to drive the soil carbon pump. Carbon Res 3(1):44. https://doi.org/10.1007/s44246-024-00132-1
Chen ZM, He LL, Ma JC, Ma JW, Ye J, Yu QG, Zou P, Sun WC, Lin H, Wang F, Zhao X, Wang Q (2024b) Long-term successive biochar application increases plant lignin and microbial necromass accumulation but decreases their contributions to soil organic carbon in rice-wheat cropping system. GCB Bioenergy 16(6):e13137. https://doi.org/10.1111/gcbb.13137
Cheng Y, Luo M, Zhang TG, Yan SH, Wang C, Deng QG, Feng H, Zhang TB, Kisekka I (2023) Organic substitution improves soil structure and water and nitrogen status to promote sunflower (*Helianthus annuus* L.) growth in an arid saline area. Agric Water Manag 283:108320. https://doi.org/10.1016/j.agwat.2023.108320
Cotrufo MF, Ranalli MG, Haddix ML, Six J, Lugato E (2019) Soil carbon storage informed by particulate and mineral-associated organic matter. Nat Geosci 12(12):989–994. https://doi.org/10.1038/s41561-019-0484-6
Cotrufo MF, Haddix ML, Kroeger ME, Stewart CE (2022) The role of plant input physical-chemical properties, and microbial and soil chemical diversity on the formation of particulate and mineral-associated organic matter. Soil Biol Biochem 168:108648. https://doi.org/10.1016/j.soilbio.2022.108648
Dong XF, Liu C, Wu XD, Man HR, Wu XW, Ma DL, Li M, Zang SY (2023) Linking soil organic carbon mineralization with soil variables and bacterial communities in a permafrost-affected tussock wetland during laboratory incubation. CATENA 221:106783. https://doi.org/10.1016/j.catena.2022.106783
Edgar R (2013) UPARSE: highly accurate OTU sequences from microbial amplicon reads. Nat Methods 10:996–998. https://doi.org/10.1038/nmeth.2604
Even RJ, Cotrufo MF (2024) The ability of soils to aggregate, more than the state of aggregation, promotes protected soil organic matter formation. Geoderma 442:116760. https://doi.org/10.1016/j.geoderma.2023.116760
Fan JP, Li FF, Fang DX, Chen QZ, Chen QK, Wang H, Pan B (2022) Effects of hydrophobic coating on properties of hydrochar produced at different temperatures: specific surface area and oxygen-containing functional groups. Bioresour Technol 363:127971. https://doi.org/10.1016/j.biortech.2022.127971
George C, Wagner M, Kücke M, Rillig MC (2012) Divergent consequences of hydrochar in the plant-soil system: arbuscular mycorrhiza, nodulation, plant growth and soil aggregation effects. Appl Soil Ecol 59:68–72. https://doi.org/10.1016/j.apsoil.2012.02.021
Heikkinen J, Keskinen R, Soinne H, Hyväluoma J, Nikama J, Wikberg H, Källi A, Siipola V, Melkior T, Dupont C, Campargue M, Larsson SH, Hannula M, Rasa K (2019) Possibilities to improve soil aggregate stability using biochar derived from various biomasses through slow pyrolysis, hydrothermal carbonization, or torrefaction. Geoderma 344:40–49
Hu YC, Su MR, Wang YF, Cui SH, Meng FX, Yue WC, Liu YF, Xu C, Yang ZF (2020) Food production in China requires intensified measures to be consistent with national and provincial environmental boundaries. Nat Food 1(9):572–582. https://doi.org/10.1038/s43016-020-00143-2
Huang X, Wang WL, Gong T, Wickell D, Kuo LY, Zhang XT, Wen JL, Kim H, Lu FC, Zhao HS, Chen S, Li H, Wu WQ, Yu CJ, Chen S, Fan W, Chen S, Bao XQ, Li L, Zhang D, Jiang LY, Khadka D, Yan XJ, Liao ZY, Zhou GK, Guo YL, Ralph J, Sederoff RR, Wei HR, Zhu P, Li FW, Ming RY, Li QZ (2024) The flying spider-monkey tree fern genome provides insights into fern evolution and arborescence. Nat Plants 10(2):344–344. https://doi.org/10.1038/s41477-024-01631-0

Huo CF, Liang JY, Zhang WD, Wang P, Cheng WX (2022) Priming effect and its regulating factors for fast and slow soil organic carbon pools: a meta-analysis. Pedosphere 32(1):140–148. https://doi.org/10.1016/s1002-0160(21)60064-4

Islam MA, Limon MSHM, Romić M (2021) Hydrochar-based soil amendments for agriculture: a review of recent progress. Arab J Geosci 102:14

Jilling A, Kane D, Williams A, Yannarell AC, Davis A, Jordan NR, Koide RT, Mortensen DA, Smith RG, Snapp SS, Spokas KA, Grandy AS (2020) Rapid and distinct responses of particulate and mineral-associated organic nitrogen to conservation tillage and cover crops. Geoderma 359:114001. https://doi.org/10.1016/j.geoderma.2019.114001

Khan TA, Saud AS, Jamari SS, Ab Rahim MH, Park JW, Kim HJ (2019) Hydrothermal carbonization of lignocellulosic biomass for carbon rich material preparation: a review. Biomass Bioenergy 130:105384. https://doi.org/10.1016/j.biombioe.2019.105384

Khosravi A, Zheng H, Liu Q, Hashemi M, Tang YZ, Xing BS (2022) Production and characterization of hydrochars and their application in soil improvement and environmental remediation. Chem Eng J 430(4):133142. https://doi.org/10.1016/j.cej.2021.133142

Krause L, Biesgen D, Treder A, Schweizer SA, Klumpp E, Knief C, Siebers N (2019) Initial microaggregate formation: association of microorganisms to montmorillonite-goethite aggregates under wetting and drying cycles. Geoderma 351:250–260. https://doi.org/10.1016/j.geoderma.2019.05.001

Kumar A, Saini K, Bhaskar T (2020) Hydochar and biochar: production, physicochemical properties and techno-economic analysis. Bioresour Technol 310:123442. https://doi.org/10.1016/j.biortech.2020.123442

Lal R, Monger C, Nave L, Smith P (2021) The role of soil in regulation of climate. Philos Trans R Soc B Biol Sci 376:1838. https://doi.org/10.1098/rstb.2021.0420

Lavallee JM, Soong JL, Cotrufo MF (2020) Conceptualizing soil organic matter into particulate and mineral-associated forms to address global change in the 21st century. Glob Change Biol 26(1):261–273. https://doi.org/10.1111/gcb.14859

Lehmann J, Kleber M (2015) The contentious nature of soil organic matter. Nature 528(7580):60–68. https://doi.org/10.1038/nature16069

Li J, Chen XH, Yu SG, Cui M (2023a) Removal of pristine and aged microplastics from water by magnetic biochar: adsorption and magnetization. Sci Total Environ 875:162647. https://doi.org/10.1016/j.scitotenv.2023.162647

Li JY, Chen P, Li ZG, Li LY, Zhang RQ, Hu W, Liu Y (2023b) Soil aggregate-associated organic carbon mineralization and its driving factors in rhizosphere soil. Soil Biol Biochem 186:109182. https://doi.org/10.1016/j.soilbio.2023.109182

Li YH, Feng XJ, Huai YB, Hassan MU, Cui ZL, Ning P (2024) Enhancing crop productivity and resilience by promoting soil organic carbon and moisture in wheat and maize rotation. Agric Ecosyst Environ 368:109021. https://doi.org/10.1016/j.agee.2024.109021

Liang C, Amelung W, Lehmann J, Kästner M (2019) Quantitative assessment of microbial necromass contribution to soil organic matter. Glob Change Biol 25(11):3578–3590. https://doi.org/10.1111/gcb.14781

Liao QH, Yuan F, Fan QY, Chen HY, Wang YM, Zhang CC, Lu C, Qiu PH, Wang CL, Zou XQ (2024) Plant- and microbial-mediated soil organic carbon accumulation in *Spartina alterniflora* salt marshes. CATENA 237:107777. https://doi.org/10.1016/j.catena.2023.107777

Liu MY, Chang QR, Qi YB, Liu J, Chen T (2014) Aggregation and soil organic carbon fractions under different land uses on the tableland of the Loess Plateau of China. CATENA 115:19–28. https://doi.org/10.1016/j.catena.2013.11.002

Ma T, Zhu SS, Wang ZH, Chen DM, Dai GH, Feng BW, Su XY, Hu HF, Li KH, Han WX, Liang C, Bai YF, Feng XJ (2018) Divergent accumulation of microbial necromass and plant lignin components in grassland soils. Nat Commun 9(1):3480. https://doi.org/10.1038/s41467-018-05891-1

Ma T, Yang ZY, Shi BW, Gao WJ, Li YF, Zhu JX, He J (2023a) Phosphorus supply suppressed microbial necromass but stimulated plant lignin phenols accumulation in soils of alpine grassland on the Tibetan Plateau. Geoderma 431:116376. https://doi.org/10.1016/j.geoderma.2023.116376

Ma YQ, Woolf D, Fan MS, Qiao L, Li R, Lehmann J (2023b) Global crop production increase by soil organic carbon. Nat Geosci 16:12. https://doi.org/10.1038/s41561-023-01302-3

Ma HH, Peng M, Yang Z, Yang K, Zhao CD, Li K, Guo F, Yang ZF, Cheng HX (2024a) Spatial distribution and driving factors of soil organic carbon in the Northeast China Plain: insights from latest monitoring data. Sci Total Environ 911:168602. https://doi.org/10.1016/j.scitotenv.2023.168602

Ma SH, Cao YD, Lu JW, Ren T, Cong RH, Lu ZF, Zhu J, Li XK (2024b) Response of soil aggregation and associated organic carbon to organic amendment and its controls: a global meta-analysis. CATENA 237:107774. https://doi.org/10.1016/j.catena.2023.107774

Mustafa A, Xu MG, Shah SAA, Abrar MM, Sun N, Wang BR, Cai ZJ, Saeed Q, Naveed M, Mehmood K, Núñez-Delgado A (2020) Soil aggregation and soil aggregate stability regulate organic carbon and nitrogen storage in a red soil of southern China. J Environ Manag 270:110894. https://doi.org/10.1016/j.jenvman.2020.110894

Naisse C, Girardin C, Lefevre R, Pozzi A, Maas R, Stark A, Rumpel C (2015) Effect of physical weathering on the carbon sequestration potential of biochars and hydrochars in soil. GCB Bioenergy 7(3):488–496. https://doi.org/10.1111/gcbb.12158

Oldfield EE, Bradford MA, Wood SA (2019) Global meta-analysis of the relationship between soil organic matter and crop yields. Soil 5(1):15–32. https://doi.org/10.5194/soil-5-15-2019

Qiao L, Wang XH, Smith P, Fan JL, Lu YL, Emmett B, Li R, Dorling S, Chen HQ, Liu SG, Benton TG, Wang YJ, Ma YQ, Jiang RF, Zhang FS, Piao SL, Müller C, Yang HQ, Hao YN, Li WM, Fan MS (2022) Soil quality both increases crop production and improves resilience to climate change. Nat Clim Change 12(6):574–280. https://doi.org/10.1038/s41558-022-01376-8

Rashid MI, Mujawar LH, Shahzad T, Almeelbi T, Ismail IMI, Oves M (2016) Bacteria and fungi can contribute to nutrients bioavailability and aggregate formation in degraded soils. Microbiol Res 183:26–41. https://doi.org/10.1016/j.micres.2015.11.007

Ren FL, Zhang RQ, Sun N, Li YL, Xu MG, Zhang FS, Xu W (2024) Patterns and driving factors of soil organic carbon sequestration efficiency under various manure regimes across Chinese croplands. Agric Ecosyst Environ 359:108723. https://doi.org/10.1016/j.agee.2023.108723

Rex D, Schimmelpfennig S, Jansen-Willems A, Moser G, Kammann C, Müller C (2015) Microbial community shifts 2.6 years after top dressing of *Miscanthus* biochar, hydrochar and feedstock on a temperate grassland site. Plant Soil 397(1–2):261–271. https://doi.org/10.1007/s11104-015-2618-y

Richter DD (2021) A world without soil: the past, present, and precarious future of the Earth beneath our feet. Science 374(6574):1452–1452. https://doi.org/10.1126/science.abm4765

Si HY, Wang R, Zhao YQ, Hao H, Zhao CK, Xing S, Yu HW, Liang XH, Lu JK, Chen XX, Wang B (2024) Large-scale soil application of hydrochar: reducing its polycylic aromatic hydrocarbon content and toxicity by heating. J Hazard Mater 471:134467. https://doi.org/10.1016/j.jhazmat.2024.134467

Six J, Elliott ET, Paustian K, Doran JW (1998) Aggregation and soil organic matter accumulation in cultivated and native grassland soils. Soil Sci Soc Am J 62(5):1367–1377. https://doi.org/10.2136/sssaj1998.03615995006200050032x

Six J, Bossuyt H, Degryze S, Denef K (2004) A history of research on the link between (micro)aggregates, soil biota, and soil organic matter dynamics. Soil till Res 79(1):7–31. https://doi.org/10.1016/j.still.2004.03.008

Sokol NW, Sanderman J, Bradford MA (2019) Pathways of mineral-associated soil organic matter formation: integrating the role of plant carbon source, chemistry, and point of entry. Glob Change Biol 25(1):12–24. https://doi.org/10.1111/gcb.14482

Song CF, Shan SD, Yang C, Zhang C, Zhou XQ, Ma Q, Yrjälä K, Zheng HB, Cao YC (2020) The comparison of dissolved organic matter in hydrochars and biochars from pig manure. Sci Total Environ 720:137423. https://doi.org/10.1016/j.scitotenv.2020.137423

Song FB, Liu KL, Lou YL, Kuzyakov Y, Wang YD (2022) Divergent responses of aggregate stability to long-term mineral and organic amendments between upland and paddy soils. J Soils Sediments 22(12):2969–2981. https://doi.org/10.1007/s11368-022-03270-4

Sonsri K, Watanabe A (2023) Insights into the formation and stability of soil aggregates in relation to the structural properties of dissolved organic matter from various organic amendments. Soil Tillage Res 232:105774. https://doi.org/10.1016/j.still.2023.105774

Sun K, Han LF, Yang Y, Xia XH, Yang ZF, Wu FC, Li FB, Feng YF, Xing BS (2020) Application of hydrochar altered soil microbial community composition and the molecular structure of native soil organic carbon in a paddy soil. Environ Sci Technol 54(5):2715–2725. https://doi.org/10.1021/acs.est.9b05864

Sun Q, Meng J, Lan Y, Shi GH, Yang X, Cao D, Chen WF, Han X (2021) Long-term effects of biochar amendment on soil aggregate stability and biological binding agents in brown earth. CATENA 205:105460. https://doi.org/10.1016/j.catena.2021.105460

Tarf OJ, Akça MO, Donar YO, Bilge S, Turgay OC, Sinag A (2022) The short-term effects of pyro-and hydrochars derived from different organic wastes on some soil properties. Biomass Convers Biorefin 12(1):129–139. https://doi.org/10.1007/s13399-021-01282-7

Tian SY, Zhu BJ, Yin R, Wang MW, Jiang YJ, Zhang CZ, Li DM, Chen XY, Kardol P, Liu MQ (2022) Organic fertilization promotes crop productivity through changes in soil aggregation. Soil Biol Biochem 165:108533. https://doi.org/10.1016/j.soilbio.2021.108533

Ul Islam M, Jiang FH, Guo ZC, Peng XH (2021) Does biochar application improve soil aggregation? A meta-analysis. Soil Tillage Res 209:104926. https://doi.org/10.1016/j.still.2020.104926

Verrone V, Gupta A, Laloo AE, Dubey RK, Hamid NAA, Swarup S (2024) Organic matter stability and lability in terrestrial and aquatic ecosystems: a chemical and microbial perspective. Sci Total Environ 906:167757. https://doi.org/10.1016/j.scitotenv.2023.167757

Wang GC, Wang MM, Guo XW, Yu YQ, Han PF, Luo ZK (2022) Efficiency of additional organic inputs for carbon sequestration in agricultural soils modulated by the priming effect and physical accessibility. Geoderma 406:115498. https://doi.org/10.1016/j.geoderma.2021.115498

Wang X, Li Z, Cheng YD, Yao H, Li H, You XW, Zhang CS, Li YQ (2023a) Wheat straw hydrochar induced negative priming effect on carbon decomposition in a coastal soil. iMeta 2(4):e134. https://doi.org/10.1002/imt2.134

Wang YY, Li H, Li YW, Guo H, Zhou J, Wang TC (2023b) Metagenomic analysis revealed sources, transmission, and health risk of antibiotic resistance genes in confluence of Fenhe, Weihe, and Yellow Rivers. Sci Total Environ 858:159913. https://doi.org/10.1016/j.scitotenv.2022.159913

Wang HG, Wang X, Zhang L, Zhang XY, Cao YB, Xiao R, Bai ZH, Ma L (2024a) Meta-analysis addressing the potential of antibiotic resistance gene elimination through aerobic composting. Waste Manag 182:197–206. https://doi.org/10.1016/j.wasman.2024.04.034

Wang R, Zheng XY, Feng ZY, Feng YH, Ying Z, Wang B, Dou BL (2024b) Hydrothermal carbonization of Chinese medicine residues: formation of humic acids and combustion performance of extracted hydrochar. Sci Total Environ 925:171792. https://doi.org/10.1016/j.scitotenv.2024.171792

Watson C, Schlösser C, Vögerl J, Wichern F (2021) Hydrochar, digestate, and process water impacts on a soil's microbial community, processes, and metal bioavailability. Soil Sci Soc Am J 85:717–731. https://doi.org/10.1002/saj2.20239

Xiao R, Wang JJ, Gaston LA, Zhou BY, Park JH, Li RH, Dodla SK, Zhan ZQ (2018) Biochar produced from mineral salt-impregnated chicken manure: fertility properties and potential for carbon sequestration. Waste Manag 78:802–810. https://doi.org/10.1016/j.wasman.2018.06.047

Xiong WJ, Luo YP, Shangguan WG, Deng Y, Li RH, Song D, Zhang MY, Li ZY, Xiao R (2024) Co-hydrothermal carbonization of lignocellulosic biomass and swine manure: optimal parameters for enhanced nutrient reclamation, carbon sequestration, and heavy metals passivation. Waste Manag 190:174–185. https://doi.org/10.1016/j.wasman.2024.09.019

Xiong WJ, Zhang MY, Wei YY, Wei YY, Song D, Luo YP, Wang JT, Cheng S, Xiao R (2025) Co-hydrothermal carbonization of lignocellulosic biomass and swine manure for humic substance abundant target products: impacts of hydrothermal temperature and feedstock composition. J Environ Chem Eng 266:242–248. https://doi.org/10.1016/j.jece.2025.116280

Yan T, Zhang ZR, Zhang Z, Wang WZ, Li D, Zhang T, Zhu ZP (2024) Applying hydrochar affects soil carbon dynamics by altering the characteristics of soil aggregates and microbes. Agronomy 14(5):1015. https://doi.org/10.3390/agronomy14051015

Yu WJ, Huang WJ, Weintraub-Leff SR, Hall SJ (2022) Where and why do particulate organic matter (POM) and mineral-associated organic matter (MAOM) differ among diverse soils? Soil Biol Biochem 172:108756. https://doi.org/10.1016/j.soilbio.2022.108756

Zhang ZZ, Wang DM, Li MX (2022) Soil respiration, aggregate stability and nutrient availability affected by drying duration and drying-rewetting frequency. Geoderma 413:115743. https://doi.org/10.1016/j.geoderma.2022.115743

Zhang J, Zhang FH, Yang L (2024) Continuous straw returning enhances the carbon sequestration potential of soil aggregates by altering the quality and stability of organic carbon. J Environ Manag 358:120903. https://doi.org/10.1016/j.jenvman.2024.120903

Zhao RN, Kuzyakov Y, Zhang HY, Wang ZR, Li TP, Shao LY, Jiang LC, Wang RZ, Li MH, Sun JX, Jiang Y, Han XG (2024) Labile carbon inputs offset nitrogen-induced soil aggregate destabilization via enhanced growth of saprophytic fungi in a meadow steppe. Geoderma 443:116841. https://doi.org/10.1016/j.geoderma.2024.116841